Separation Science and Technology
Publication details, including instructions for authors and subscription information:
http://www.informaworld.com/smpp/title~content=t713708471

Modeling Study of the Influence of Porosity on Membrane Absorption Process

Geng Chen[a]; Zhongqi Ren[a]; Weidong Zhang[a]; Jian Gao[a]
[a] State Key Laboratory of Chemical Resource Engineering, Beijing University of Chemical Technology, Beijing, People's Republic of China

To cite this Article Chen, Geng , Ren, Zhongqi , Zhang, Weidong and Gao, Jian(2007) 'Modeling Study of the Influence of Porosity on Membrane Absorption Process', Separation Science and Technology, 42: 15, 3289 — 3306
To link to this Article: DOI: 10.1080/01496390701626644
URL: http://dx.doi.org/10.1080/01496390701626644

Separation Science and Technology, 42: 3289–3306, 2007

ISSN 0149-6395 print/1520-5754 online
DOI: 10.1080/01496390701626644

Modeling Study of the Influence of Porosity on Membrane Absorption Process

Geng Chen, Zhongqi Ren, Weidong Zhang, and Jian Gao
State Key Laboratory of Chemical Resource Engineering, Beijing University of Chemical Technology, Beijing, People's Republic of China

Abstract: A theoretical model based on the advancing front model was developed to analyze the influence of porosity on membrane absorption process. Perturbation solutions were obtained and a nonlinear transformation was applied to increase the accuracy of the solutions. The concentration profile of the solute in the liquid side near the membrane surface was simulated for different operation conditions. The influencing factors on the diffusing rate of the solute concentration profile were analyzed qualitatively. In the case of the rapid mass transfer system, the time of reaction front to reach the midpoint of two proximate pores is relatively long, which means that the concentration layer of solute overcasts the whole surface of membrane slowly, there is a "dead" area for mass transfer, so the influence of porosity should be taken into account. In the case of slow mass transfer system, the time can be ignored compared with the overall experiment time, and the influence of porosity is negligible. The absorption rates were calculated based on the developed model and the calculated results agreed well with the literature results.

Keywords: Gas absorption, porosity, mass transfer, mathematical model, porous membrane

INTRODUCTION

Membrane absorption process is a kind of coupling technology combining membrane separation with the conventional absorption process, which can

Received 14 February 2007, Accepted 13 June 2007
Address correspondence to Weidong Zhang, State Key Laboratory of Chemical Resource Engineering, College opf Chemical Engineering, Beijing University of Chemical Technology, P. O. Box 1#, Beijing 100029, People's Republic of China. Tel.: + 86-010-6442-3628; E-mail: zhangwd@mail.buct.edu.cn

effectively overcome the conflict between selectivity and flux in the membrane process, and eliminate the drawbacks associated with the conventional absorption such as flooding (1). Gas membrane absorption system was first emerged as blood oxygenators (2). Zhang Qi and Cussler (3, 4) investigated the absorption of several kinds of gases in hydrophobic micro-porous hollow fiber membrane contactors in 1985. Since then, membrane absorption has been studied extensively, including mass transfer mechanism, mathematical model, operation modes, flow status, materials of membrane, various absorbents and so on (5–14).

In these processes, polymeric micro-porous membranes were applied to separate the gas phase and liquid phase. Unlike the gas membrane separation process using non-porous membranes (15), the membranes themselves usually do not offer any selectivity, simply providing a support for the interface at which the two phases making contact in the pore. The membrane is a major component of the system and it constitutes another additional resistance to mass transfer, compared with a conventional gas absorption system (3, 16). Early in 1985, Zhang Qi (3) had reckoned that the existence of a micro-porous membrane made a reduction of the mass transfer area. In many studies on the membrane absorption process, resistance-in-series model has been used to describe the mass transfer process. In these models, membrane micro-structure characteristics are incorporated into only one phenomenological parameter, the resistance of membrane phase (17), while in some cases, i.e., when pure CO_2 was used like this study, the membrane phase resistance can be ignored. So, these models do not explicitly take into account the parameters like porosity.

Little attention has been paid to the influence of porosity on mass transfer in the membrane absorption processes, and the concerned viewpoints were conflicted or controversial. Kreulen et al. (7, 18) confirmed that the membrane micro-structure characteristics did not affect the mass transfer. In contrast, Kim and Yang (10) elicited the theoretical model which agreed well with their experimental results, using the total area of pores as effective mass transfer area. Huseni and Rangwala (19) used a hollow fiber membrane with a porosity of 30% for the absorption of carbon dioxide, and point out that the ratio of the effective mass transfer area to the whole membrane area was 0.58, which means the effective mass transfer area is not the total area of pores nor the membrane surface. This is different from the conclusions of Kreulen (7, 18) and Kim (10). Evren (20) separated the whole membrane into “TD zone” (transfer and diffusion zone) and “D zone” (diffusion zone). It was figured that gas transferred to the absorbent and diffused above the pores, but only diffusion occurred above the membrane polymeric body. However, only one kind of membrane with a porosity of 38% was used in his experiment.

It is extensively accepted that the mass transfer coefficient will increase with the increasing of membrane porosity, which means the increase of real bi-phase contact area. However, Zhang Xiuli (21) and Zhang Zeting (22)

studied the mass transfer performances of carbon dioxide absorbed by water or NaOH aqueous through micro-porous expanded polytetrafluoroethylene (ePTFE) flat membrane, it was found that the membrane porosity had little effect on the mass transfer performance of the liquid phase for the CO_2-water system, but had a significant effect for the CO_2-NaOH aqueous system. The results were explained by illustration, they pointed out that the different mass transfer characters are due to the concentration profile in the liquid phase, the ratio of the "dead" area for mass transfer to overall membrane area is related to the membrane porosity and the absorption rate. The influence of porosity almost can be negligible when the solute concentration profile overcast the membrane surface on the liquid side that is to say the influence of porosity can be ignored after the solute concentration profile diffused over the midpoint of proximate pores. Simulation and theory are necessary for further understanding of the experiment results.

In this work, the influencing factors on the solute concentration profile were analyzed qualitatively. A theoretical model based on advancing front model (23) was presented to analyze the effect of porosity on the membrane absorption process. According to the rate of the solute concentration layer to overcast the whole surface of the membrane, the influence of porosity can be determined. And the absorption rates were calculated based on the model developed in this study.

MATHEMATICAL MODEL

Model Development

In the absorption model, flat membranes were employed to avoid the influence of the non-ideal flow in the shell side of hollow fiber module. The carbon dioxide gas phase, which kept a constant pressure, was absorbed by sodium hydroxide aqueous or de-ionized water. Both the gas and liquid phase were all immobile, so that the influence of liquid flow can be avoided.

The solute concentration at the gas/liquid interface is presumed to follow Henry's law $c^* = pH$. And the reaction between carbon dioxide and hydroxyl ion is presupposed to be instantaneous and irreversible in the mol ratio of 1:1. When pure water is used as absorbent, the concentration of hydroxyl ion in liquid phase can be calculated as $10^{-7}\ \mathrm{mol} \cdot \mathrm{L}^{-1}$.

In general, micro-pores which are distributed on the membrane exhibit non-uniform sizes and shapes. For predigestion of the model, the structure of micro-porous membranes can be assumed as repeats of a columnar pore and a polymeric body with invariant size (20), which is shown in Fig. 1(a). It is assumed that the micro-pores in the membranes are not wetted.

According to the advancing front model (23), there exists a sharp boundary, or reaction front, at which the reaction takes place, and which separates the inner region containing no hydroxyl ion from the outer region

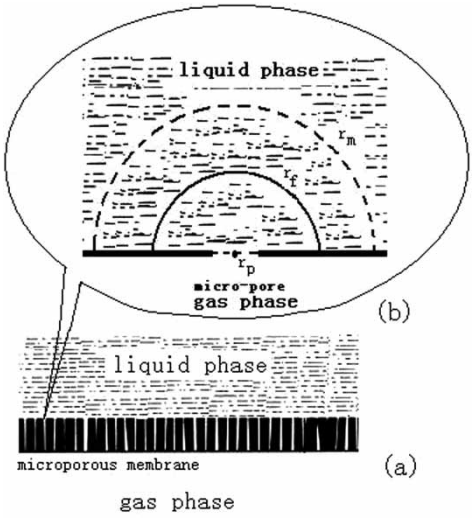

Figure 1. Schematic representation of the advancing front model.

which contains no solute (carbon dioxide), as depicted in Fig. 1(b). Carbon dioxide taken up from the gas phase diffuses through the inner region to the reaction front, where it reacts with hydroxyl ion. The diffusion of the reaction products and absorbent are assumed to be negligible. As the absorbent is consumed by the reaction, this reaction front advances inwards towards the interior of the liquid phase.

Mathematical Description

The gas phase is pure carbon dioxide and the gas pressure was maintained constant, so there could be no resistance to mass transfer in the gas side or in the pores. On the assumptions that Henry's law coefficient and diffusion coefficient were obtained from literature (22) and are invariable, the concentration of carbon dioxide in the inner region can be predicted by Eq. (1). For the simplification of calculation, the gas/liquid interface is presumed to be a hemispherical face with the radius r_p.

$$\frac{\partial c}{\partial t} = D\left[\frac{1}{r}\frac{\partial^2}{\partial r^2}(rc)\right] \quad (r_p \le r \le r_f) \tag{1}$$

$$t = 0 \quad c = 0 \quad (r > r_p)$$
$$r = r_p \quad c = c^* \quad (t > 0)$$
$$r = r_f \quad c = 0 \quad (t > 0)$$

A material balance over the reaction front can be written as

$$c_{OH^-}\frac{dr_f}{dt} = -D\left.\frac{\partial c}{\partial r}\right|_{r=r_f} \quad t=0 \quad r_f = r_p \tag{2}$$

The equations can be changed into normalized dimensionless form by defining dimensionless parameters as follows.

$$\theta = \frac{c^* - c}{c^*} \quad R = \frac{r}{r_p} \quad R_f = \frac{r_f}{r_p} \quad \in = \frac{c^*}{c_{OH^-}} \quad \tau = \in \frac{Dt}{r_p^2} \tag{3}$$

Then the boundary-value problem in its normalized form will be yielded.

$$\in \frac{\partial\theta}{\partial\tau} = \frac{1}{R}\frac{\partial^2(R\theta)}{\partial R^2} \quad (1 \le R \le R_f) \tag{4}$$

$$R > 1 \quad \theta = 1 \quad (\tau = 0)$$
$$R = 1 \quad \theta = 0 \quad (\tau > 0)$$
$$R = R_f \quad \theta = 1 \quad (\tau > 0)$$

and

$$\frac{dR_f}{d\tau} = \left.\frac{\partial\theta}{\partial R}\right|_{R=R_f} \tau = 0 \quad R_f = 1 \tag{5}$$

Combining with Eq. (5), the independent variables of Eq. (4) can be changed from (R, τ) to (R, R_f).

$$\frac{1}{R}\frac{\partial^2(R\theta)}{\partial R^2} = \in \frac{\partial\theta}{\partial R_f}\left.\frac{\partial\theta}{\partial R}\right|_{R=R_f} \quad (1 \le R \le R_f) \tag{6}$$

$$\theta(R=1,\, R_f) = 0 \quad \theta(R=R_f,\, R_f) = 1$$

These equations are inherently non-linear, and can not be solved analytically. However, they can be solved by perturbation methods (24). The parameter $\in$ can be taken to serve as the perturbation parameter. Here, assume the perturbation solution in terms of $\in$ as follows:

$$\theta = \theta_0 + \in \theta_1 + \in^2 \theta_2 \tag{7}$$

Substituting Eq. (7) into Eq. (6), the perturbation equations can be found by collecting terms in equal powers of $\in$.
Terms of order $\in^0$:

$$\frac{1}{R}\frac{\partial^2(R\theta_0)}{\partial R^2} = 0 \tag{8}$$

$$\theta_0(R=1,\, R_f) = 0, \quad \theta_0(R=R_f,\, R_f) = 1$$

Terms of order $\in^1$:

$$\frac{1}{R}\frac{\partial^2(R\theta_1)}{\partial R^2} = \frac{\partial\theta_0}{\partial R_f}\frac{\partial\theta_0}{\partial R}\bigg|_{R=R_f} \tag{9}$$

$$\theta_1(R=1,\ R_f)=0, \quad \theta_1(R=R_f,\ R_f)=0$$

Terms of order $\in^2$:

$$\frac{1}{R}\frac{\partial^2(R\theta_2)}{\partial R^2} = \frac{\partial\theta_0}{\partial R_f}\frac{\partial\theta_1}{\partial R}\bigg|_{R=R_f} + \frac{\partial\theta_1}{\partial R_f}\frac{\partial\theta_0}{\partial R}\bigg|_{R=R_f} \tag{10}$$

$$\theta_2(R=0,\ R_f)=0, \quad \theta_2(R=R_f,\ R_f)=0$$

Then the solutions to the three equations above can be worked out. Zero-order solution:

$$\theta_0 = \frac{1-1/R}{1-1/R_f} \tag{11}$$

First-order solution:

$$\theta_1 = \frac{R_f-2}{6(R_f-1)^3}\left(1-\frac{1}{R}\right) - \frac{R^2-3R+2}{6R_f(R_f-1)^3} \tag{12}$$

Second-order solution:

$$\begin{aligned}\theta_2 = {} & \frac{-12R_f^5+53R_f^4-85R_f^3+60R_f^2-8R_f-8}{360R_f^2(R_f-1)^6}\left(1-\frac{1}{R}\right) \\ & + \frac{R_f+2}{36R_f^2(R_f-1)^5}(R^2-3R+2) \\ & + \frac{4R_f-1}{360R_f^3(R_f-1)^5}(3R^4-15R^3+20R^2-8)\end{aligned} \tag{13}$$

Eq. (5) can be written as Eq. (14) by substituting Eq. (7) in it.

$$\frac{dR_f}{d\tau} = \frac{\partial\theta_0}{\partial R}\bigg|_{R=R_f} + \in \frac{\partial\theta_1}{\partial R}\bigg|_{R=R_f} + \in^2 \frac{\partial\theta_2}{\partial R}\bigg|_{R=R_f} \tag{14}$$

Substituting Eqs. (11–13) into Eq. (14) and rearranging it, Eq. (15) is elicited.

$$\frac{dR_f}{d\tau} = \frac{1}{R_f(R_f-1)}\left(1- \in \frac{1}{3R_f} + \in^2 \frac{1+6R_f}{45R_f^3}\right) \tag{15}$$

Separating the variables, then integrating Eq. (15) and substituting the boundary conditions, the solution to τ is given.

$$\tau = \frac{3(R_f - 1)^2 + 2(R_f - 1)^3}{6} + \in \frac{1}{6}(R_f - 1)^2 - \in^2 \frac{1}{45}\frac{(R_f - 1)^2}{R_f} \tag{16}$$

It can be seen from Fig. 1(a) that the distance between the center of a pore and the midpoint of the two proximate pores could be calculated by Eq. (17).

$$r_m = \frac{r_p}{\varepsilon} \tag{17}$$

So the dimensionless distance is

$$R_m = \frac{r_m}{r_p} = \frac{1}{\varepsilon} \tag{18}$$

The overall absorption rate before the reaction front reaches the midpoint of the two proximate pores can be calculated by Eq. (19).

$$N_t = -D\frac{\partial c}{\partial r}\bigg|_{r=r_p} \times 2\pi r_p^2 \times \frac{A_{membrane}\varepsilon}{A_{pore}} = \frac{2Dc^* A_{membrane}\varepsilon}{r_p}\frac{\partial \theta}{\partial R}\bigg|_{R=1} \tag{19}$$

When the influence of porosity is negligible, the influence caused by the existence of membrane can be ignored, which means direct gas/liquid contact. The absorption rate can be written as

$$N_t = \frac{2Dc^* A_{membrane}}{r_p}\frac{\partial \theta}{\partial R}\bigg|_{R=1} \tag{20}$$

EXPERIMENT

In this experiment, pure carbon dioxide (gas phase) continuously flowed into the flat module during the absorption process, and the absorbent was either deionized water or 0.1 M NaOH solution. Experimental setup is shown in Fig. 2. Three kinds of expanded polytetrafluoroethylene (ePTFE) flat membranes in Table 1 were employed. The detailed operation method and parameters can be obtained from the reference literature (22).

RESULTS AND DISCUSSION

Modification of the Perturbation Solutions

The accuracy of the perturbation solution is related to the values taken on by the parameter. It is usually possible to calculate only the first few terms of the

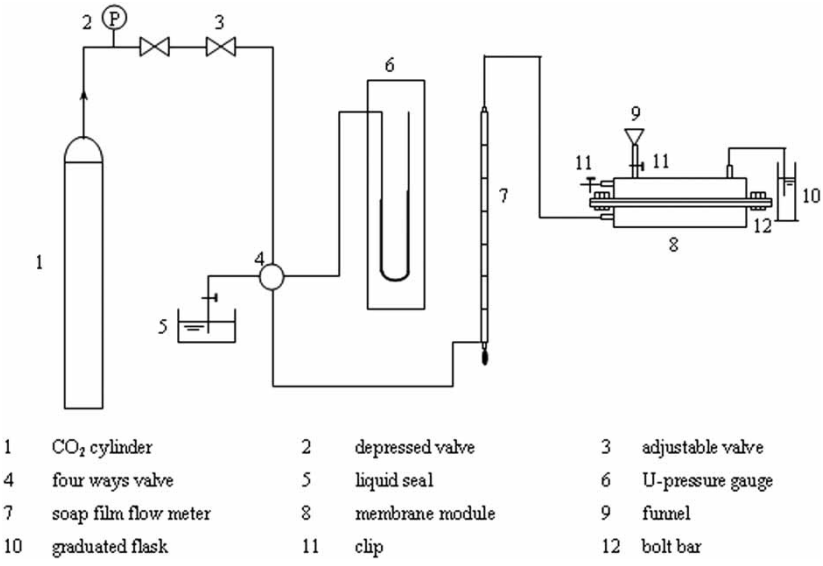

Figure 2. The experimental setup.

perturbation solution because of the algebraic complexity. And if properly used, a great amount of information will be yielded from the first few terms.

The normalized concentration distributions obtained from the perturbation solution (θ_1^f, θ_2^f) at a normalized reaction front position $R_f = 2$ are shown in Fig. 3. And the normalized time solutions (τ_1^f,τ_2^f) are shown in Fig. 4. The first-order and second-order solutions for various values of $\in$ are shown in these figures. When $\in = 0.5$, these solutions are almost superposed. But as the value of $\in$ increasing, the disparity between the first- and second-order solutions becomes more explicit. Especially when $\in = 100$, the second-order solutions become minus because only the first three terms of solution have been calculated but the posterior terms are truncated.

Shanks (25) advocated a series of non-linear sequence-to-sequence transformation, which are very useful when the perturbation series is slowly convergent or divergent. Since only the first three terms have been calculated

Table 1. Mricro-structural parameters of membranes

	Mean pore radius (10^{-7} m)	Surface porosity	Surface area (m^2)
1#	2.0	89.1%	0.045
2#	2.0	68.2%	0.045
3#	2.0	50.5%	0.045

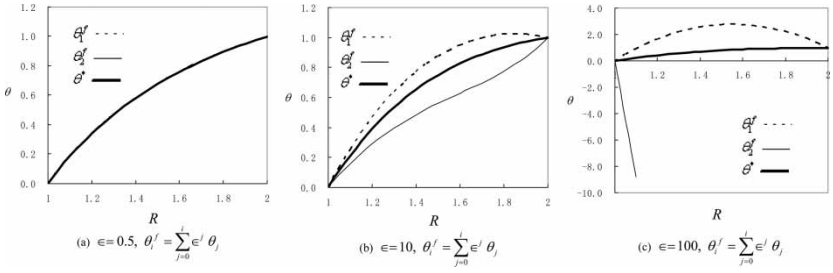

Figure 3. Normalized concentration distributions at a normalized reaction front position $R_f = 2$.

in Eq. (7), the simplest non-linear transformations can be applied to get the result of the normalized concentration distribution.

$$\theta^* = \frac{\theta_0\theta_1 - \in(\theta_0\theta_2 - \theta_1^2)}{\theta_1 - \in\theta_2} = \theta_0 \frac{1 + \in/R_f^2\{1/6 + (4R_f - 1)/20[1 + (R/R_f)^2\theta_0^2] + 1/6[1 - (R/R_f)^2\theta_0^2]\}}{1 + \in/R_f^2\{1/6 + (4R_f - 1)/20[1 + (R/R_f)^2\theta_0^2]\}} \tag{21}$$

The same transformation can be applied to the terms in Eq. (16), yielding for the normalized time.

$$\tau^* = \frac{\tau_0\tau_1 - \in(\tau_0\tau_2 - \tau_1^2)}{\tau_1 - \in\tau_2} = \frac{1 - 3R_f^2 + 2R_f^3 + \in[2/15(1 - 3R_f^2 + 2R_f^3)/R_f + (R_f - 1)^2]}{6 + (4/5)(\in/R_f)} \tag{22}$$

Pedroso and Domoto (26) had demonstrated these transformations and found that the transformed solutions were more accurate. The first- and

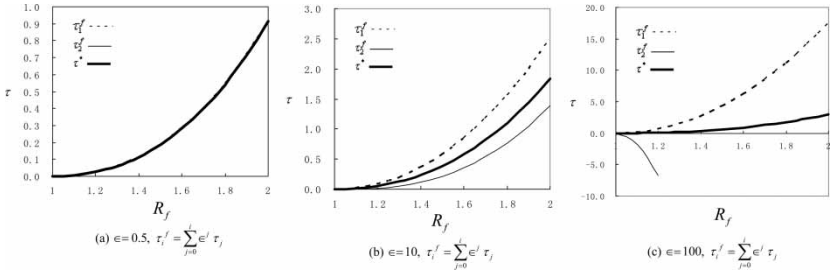

Figure 4. Normalized time solutions as a function of the normalized reaction front position.

second-order solutions have the opposite sign, suggesting that the exact solutions will probably be found between these two solutions. The nonlinear transformed solutions θ^* and τ^* are shown as well in Fig. 3 and Fig. 4. The curves of the transformed solutions are always found to be between those of the first- and second-order solutions. This result means that θ^* and τ^* can be used in the following discussion, and the accuracy is satisfactory.

Position of the Reaction Front

When the liquid phase is kept stable, the concentration distribution of the solute in the liquid phase changes with time. So the position of the reaction front is time-dependent according to the assumption of the advancing front model. The normalized positions of the reaction front can be calculated by iteration in Eq. (22).

The effects of absorbent concentration and gas pressure on the position of reaction front at normalized time $\tau^*/\in = 115$, are shown in Fig. 5 and Fig. 6 respectively. The results in Fig. 5 show that the dimensionless position of the reaction front at the normalized time $\tau^*/\in = 115$ decreases as the absorbent concentration increases. When the absorbent concentration increases, more hydroxyl ions exist in unit volume, and more carbon dioxide can be consumed, so the advancing rate of reaction front is slowed up. It is shown in Fig. 6 that the dimensionless position of the reaction front increases along with the increase of gas pressure. This is because the concentration of the solute at the gas/liquid interface increases with the increasing of gas pressure according to Henry's law, so the driving force for mass transfer becomes bigger.

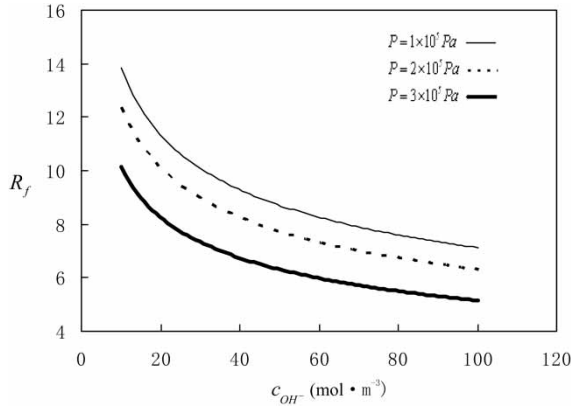

Figure 5. Normalized position of reaction front at the normalized time $\tau^*/\in = 115$ as a function of the absorbent concentration.

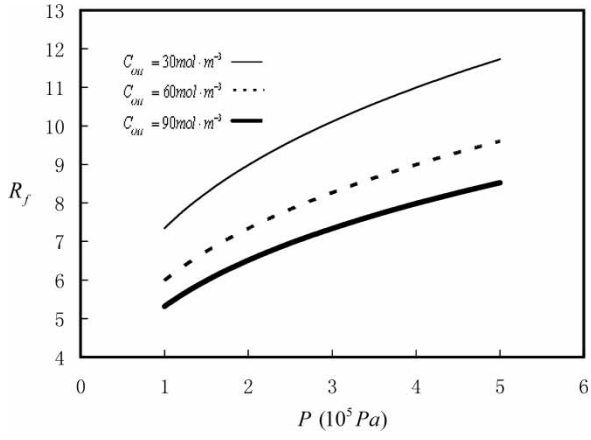

Figure 6. Normalized position of reaction front at the normalized time $\tau^*/\in = 115$ as a function of the gas pressure.

The value of perturbation parameter $\in$ is determined by the pressure of the gas phase and the concentration of absorbent. So $\in$ can be regarded as a qualitative measure of the advancing rate of reaction front. The position of reaction front at the normalized time $\tau^*/\in = 115$ is shown in Fig. 7 as a function of $\in$. Results mean that the advancing rate of reaction front increases with the increase of gas pressure, but decreases with the increase of absorbent concentration. Accordingly, it can be recognized that the advancing rate of the reaction front increases with the increasing of $\in$.

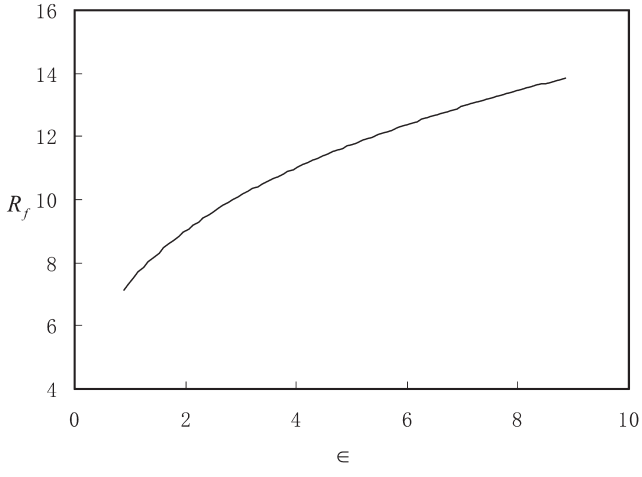

Figure 7. Normalized position of reaction front at the normalized time $\tau^*/\in = 115$ as a function of $\in$.

Effect of Porosity on Absorption Process

As described by Zeting Zhang (22), there are transfer zones and non-transfer zones near the membrane surface on the liquid side. Before the reaction front reaches the midpoint of two proximate pores, the hemispherical concentration profile of solute does not cover the whole surface of the membrane, so there are "dead" areas for mass transfer. Within the "dead" areas, no mass transfer occurs since the solute concentration is zero out of the advancing front. When the reaction front reaches the midpoint and overlays each other, the layer of solute overcasts the whole surface of the membrane, the solution concentration near the membrane surface can be considered to be homogeneous, so the effect of porosity becomes weakened or even disappears.

The normalized time $\tau^*/\in$, which is consumed for the reaction front to reach the midpoint of two proximate pores, is denoted by τ_m. The calculated τ_m for various porosities are shown in Fig. 8 and Fig. 9 as a function of absorbent concentration and gas pressure respectively. The value of τ_m increases as absorbent concentration increases, and decreases when gas pressure increases. This is coincident with the conclusion above that the advancing rate of the reaction front increases with the decreasing of the absorbent concentration or the increasing of gas pressure.

When low absorbent concentration or high gas pressure are applied, the layer of the solute overcast the whole surface of the membrane fast. Compared with the whole experiment time, the period for the concentration profile to overcast the whole membrane surface is too small to be influential, so the influence of porosity is little. On the can contrary, when high absorbent concentration or low gas pressure are applied, the reaction front reaches the

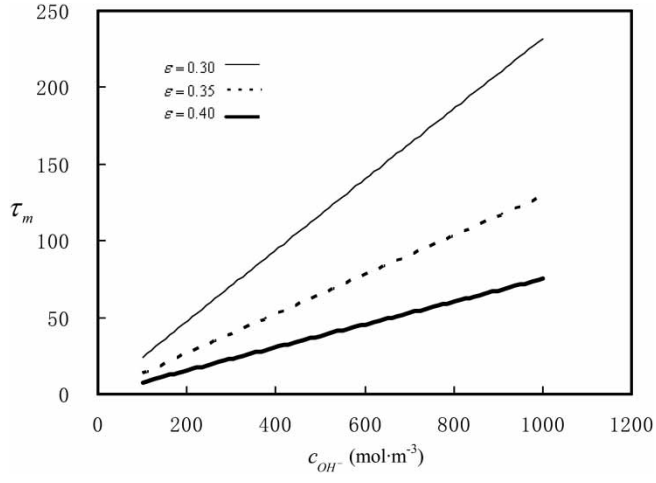

Figure 8. Normalized time consumed for the reaction to reach the midpoint of two proximate pores as a function of the absorbent concentration ($p = 1$ atm).

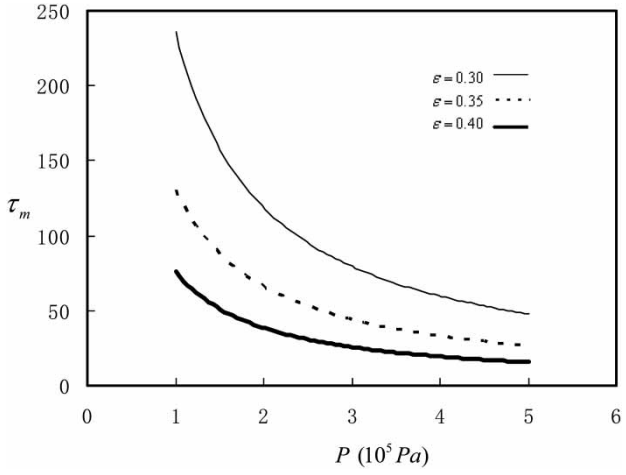

Figure 9. Normalized time consumed for the reaction to reach the midpoint of two proximate pores as a function of the gas pressure ($C_{OH^-} = 1000$ mol · m^{-3}).

midpoint of proximate membrane pores slowly, there exist "dead" areas for mass transfer, so the influence of porosity become visible. Just as the experiment data of our previous work (22), the effect of porosity on the membrane absorption process is seriously in the "fast transfer" system but little in the "slow transfer" system.

Figure 10 shows how the normalized time τ_m depends on the porosity of membrane when the perturbation parameter $\in = 0.3$. It can be seen that the

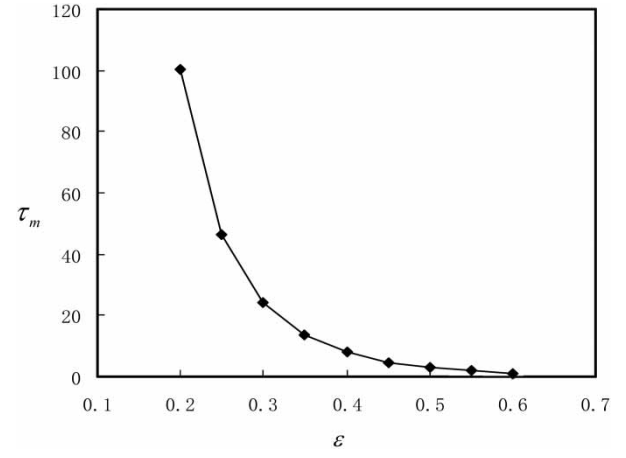

Figure 10. Normalized time consumed for the reaction to reach the midpoint of two proximate pores as a function of the porosity ($\in = 0.3$).

value of τ_m decreases sharply when the porosity increases. This means the influence of porosity is relatively small when the porosity is bigger. This is due to the shorter distance between two proximate pores when the porosity becomes big.

In the event that the time τ_m is comparative to or more than the overall experiment time, which means that the reaction front does not reach the midpoint before the experiment is finished, the effect of porosity must be taken into account. Therefore, the overall absorption rate can be calculated by Eq. (19).

If the time τ_m counts for little compared with the overall experiment time, it can be ignored. That is to say, if the layer of solute overcast the whole surface of membrane in a short time, no "dead" area for mass transfer exists, so the effect of porosity can be ignored. In this case, the overall absorption rate can be calculated by Eq. (20).

Calculation of Absorption Rate

In the process of model calculation, the diffusion of hydroxyl ion is ignored. In fact, the diffusion of hydroxyl ion into the reaction front will slow the advancing rate of the reaction front and accelerate the absorption. That is to say, the concentration of hydroxyl ion is not constant in the actual case, it is time-dependent. Accordingly, the perturbation parameter $\in$ is a function of time. The absorption rate can be calculated by fitting the function of $\in = f(t)$ and substituting it into Eqs. (19) and (20).

The calculated absorption rates are shown in Fig. 11 and Fig. 12 compared with the experiment results. According to the results of Zhang

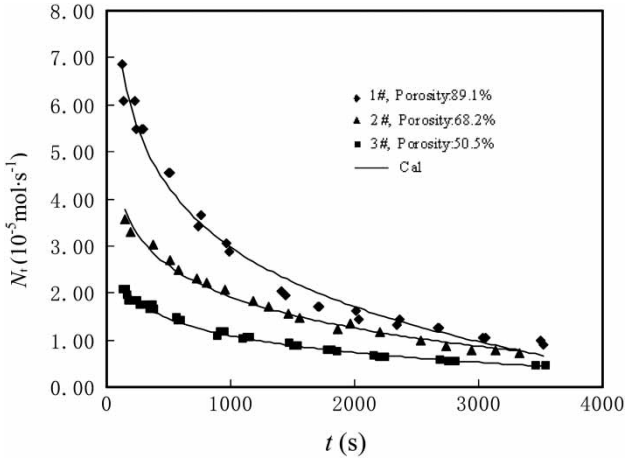

Figure 11. Absorption rate as a function of time (0.1 M NaOH solution as absorbent).

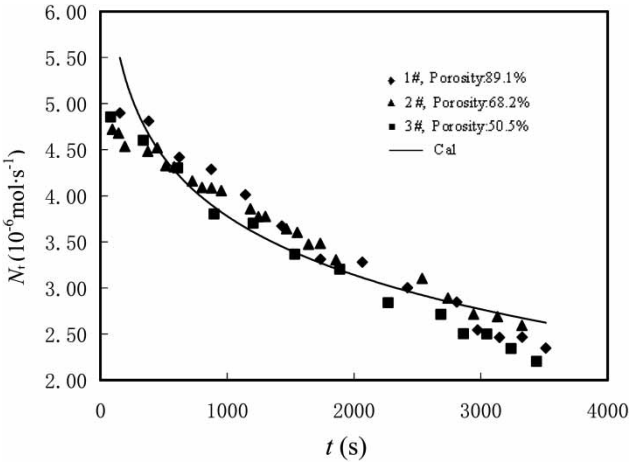

Figure 12. Absorption rate as a function of time (pure water as absorbent).

Zeting (22), the effect of membrane porosity is more obvious in the prior time-interval, so only the absorption rates in the prior 3600 seconds are shown. When 0.1 M NaOH solution is used as an absorbent, the membrane porosity has a prominent effect on the absorption process, but the effect is little when pure water serves as absorbent.

CONCLUSIONS

The nonlinear system of equations was derived based on the advancing front model (23) to describe the unsteady process of membrane absorption. Perturbation solutions were obtained and a nonlinear transformation was applied to increase the accuracy of the solutions.

The position of the reaction front was calculated as a function of time. The advancing rate of the reaction front increases with the increasing of gas pressure, but decreases with the increasing of the absorbent concentration. So the perturbation parameter $\in$ can be regarded as a qualitative measure of the advance rate of reaction front. It can be recognized from the results that the advancing rate of reaction front increases with the increase of $\in$.

The influence of membrane porosity on the absorption process can be determined according to the time for the reaction front to reach the midpoint of two proximate pores. If the time is relatively long, this means that the concentration layer of the solute overcasts the whole surface of the membrane slowly, so the influence of membrane porosity should be taken into account. In case the time can be ignored compared with the overall experiment time, the influence of the membrane porosity is negligible. Perturbation

methods usually give an accurate enough solution at small values of the perturbation parameter. At the same time, the effect of porosity is present only at small values of the perturbation parameter, which makes the derived solution adequate for analyzing the effect of porosity. Absorption rates were calculated based on the developed model and the calculated results agreed well with the literature results.

NOMENCLATURE

$A_{membrane}$	overall area of membrane (m^2)
A_{pore}	cross-section area of micro-pore (m^2)
C	concentration of CO_2 ($mol \cdot m^{-3}$)
c^*	equilibrium concentration of CO_2 at the gas/liquid interface ($mol \cdot m^{-3}$)
c_{OH^-}	concentration of hydroxyl ion ($mol \cdot m^{-3}$)
D	diffusion coefficient of CO_2 ($m^2 \cdot s^{-1}$)
H	Henry's constant of CO_2 ($mol \cdot m^{-3} \cdot Pa^{-1}$)
N_t	absorption rate of CO_2 ($mol \cdot s^{-1}$)
P	pressure of the gas phase
R	normalized dimensionless radial position as defined in Eq. (3)
R_f	normalized dimensionless position of the reaction front as defined in Eq. (3)
R_m	normalized dimensionless distance between the center of a pore and the midpoint of two proximate pores as defined in Eq. (18)
r	radial position (m)
r_f	position of the reaction front (m)
r_m	distance between the center of a pore and the midpoint of two proximate pores (m)
r_p	mean radius of micro-pore on the membrane (m)
t	time (s)
t_a	overall experiment time (s)
t_m	time for the reaction front to reach the midpoint of two proximate pores (s)

Greek Letters

ε	porosity of membrane
$\in$	perturbation parameter as defined in Eq. (3)
θ	normalized dimensionless concentration of CO_2 as defined in Eq. (3)
θ^*	modified solution to normalized concentration distribution as defined in Eq. (21)

θ_1^f	the first-order solution to normalized concentration distri bution as defined in Fig. 3
θ_2^f	the second-order solution to normalized concentration distribution as defined in Fig. 3
τ	normalized dimensionless time as defined in Eq. (3)
τ^*	modified solution to normalized time as defined in Eq. (22)
τ_m	normalized dimensionless time for the reaction front to reach the midpoint of two proximate pores
τ_1^f	the first-order solution to normalized time as defined in Fig. 4
τ_2^f	the second-order solution to normalized time as defined in Fig. 4

ACKNOWLEDGMENTS

This work was supported by the National Natural Science Foundation of China (No. 20206002) and the Beijing NOVA Program (H013610250112).

REFERENCES

1. Richard, W.B. (2000) *Membrane Technology and Applications*, 1st edn.; McGraw-Hill: New York.
2. Esato, K. and Eiseman, B. (1975) Experimental evaluation of Gore-Tex membrane oxygenator. *Journal of Thoracic and Cardiovascular Surgery*, 69: 690–697.
3. Zhang, Qi. and Cussler, E.L. (1985) Microporous hollow fibers for gas absorption: I. Mass transfer in the liquid. *Journal of Membrane Science*, 23 (3): 321–332.
4. Cussler, E.L. and Zhang, Qi. (1985) Microporous hollow fibers for gas absorption: II. Mass transfer across the membrane. *Journal of Membrane Science*, 23 (3): 333–345.
5. Cooney, D.O. and Jackson, C.C. (1989) Gas absorption in a hollow fibre device. *Chemical Engineering Communications*, 179: 153–163.
6. Littel, R.J., Filmer, B., Versteeg, G.F., and Van Swaaij, W.P.M. (1991) Modelling of simultaneous absorption of H_2S and CO_2 in alkanolamine solutions: The influence of parallel and consecutive reversible reactions and the coupled diffusion of ionic species. *Chemical Engineering Science*, 46 (9): 2303–2313.
7. Kreulen, H., Smolders, C.A., Versteeg, G.F., and Van Swaaij, W.P.M. (1993) Microporous hollow fibre membrane modules as gas-liquid contactors. Part 1. Physical mass transfer processes. *Journal of Membrane Science*, 78 (3): 197–216.
8. Kreulen, H., Smolders, C.A., Versteeg, G.F., and Van Swaaij, W.P.M. (1993) Microporous hollow fibre membrane modules as gas-liquid contactors Part 2. Mass transfer with chemical reaction. *Journal of Membrane Science*, 78 (3): 217–238.
9. Federspiel, W.J., William, J.L., and Hattler, B.G. (1996) Gas flow dynamics in hollow-fiber membranes. *AIChE Journal*, 42 (7): 2094–2099.

10. Kim, Y.S. and Yang, S.M. (2000) Absorption of carbon dioxide through hollow fiber membranes using various aqueous absorbents. *Separation and Purification Technology*, 21 (1–2): 101–109.
11. Wang, R., Li, D.F., and Liang, D.T. (2004) Modeling of CO_2 capture by three typical amine solutions in hollow fiber membrane contactors. *Chemical Engineering and Processing*, 43 (7): 849–856.
12. Dindore, V.Y., Brilman, D.W.F., and Versteeg, G.F. (2005) Hollow fiber membrane contactor as a gas-liquid model contactor. *Chemical Engineering Science*, 60 (2): 467–479.
13. De Montigny, D., Tontiwachwuthikul, P., and Chakma, A. (2006) Using polypropylene and polytetrafluoroethylene membranes in a membrane contactor for CO_2 absorption. *Journal of Membrane Science*, 277 (1–2): 99–107.
14. Todorovic, J., Krstic, D.M., Vatai, G.N., and Tekic, M.N. (2006) Gas absorption in a hollow-fiber membrane contactor with pseudo-plastic liquid as an absorbent. *Desalination*, 193 (1–3): 286–290.
15. Quinn, R. and Laciak, D.V. (1997) Polyelectrolyte membranes for acid gas separations. *Journal of Membrane Science*, 131 (1–2): 49–60.
16. Mavroudi, M., Kaldis, S.P., and Sakellaropoulos, G.P. (2006) A study of mass transfer resistance in membrane gas-liquid contacting processes. *Journal of Membrane Science*, 272 (1–2): 103–115.
17. Iversen, S.B., Bathia, V.K., Dam-Johansen, K., and Jonsson, G.E. (1997) Characterization of microporous membranes for use in membrane contactors. *Journal of Membrane Science*, 130 (1–2): 205–217.
18. Kreulen, H., Smolders, C.A., Versteeg, G.F., and Van Swaaij, W.P.M. (1993) Determination of mass transfer rates in wetted and non-wetted microporous membranes. *Chemical Engineering Science*, 48 (11): 2093–2102.
19. Rangwala, H.A. (1996) Absorption of carbon dioxide into aqueous solutions using hollow fiber membrane contactors. *Journal of Membrane Science*, 112 (2): 229–240.
20. Evren, V. (2000) A numerical approach to the determination of mass transfer performances through partially wetted microporous membranes: transfer of oxygen to water. *Journal of Membrane Science*, 175 (1): 97–110.
21. Zhang, X.L., Zhang, W.D., Hao, X.M., Zhang, H.F., and Zhang, Z.T. (2005) Mathematical model of gas absorption for PTFE membrane and the effect of porosity. *Journal of Chemical Engineering of Chinese Universities*, 19 (4): 427–432.
22. Zhang, Z.T., Gao, J., Zhang, W.T., and Ren, Z.Q. (2006) Experimental study of the effect of membrane porosity on membrane absorption process. *Separation Science and Technology*, 41 (14): 3245–3263.
23. Ho, W.S., Hatton, T.A., Lightfoot, E.N., and Li, N.N. (1982) Batch extraction with liquid surfactant membranes: A diffusion controlled model. *AIChE Journal*, 28 (4): 662–670.
24. Nayfeh, A.H. (1973) *Perturbation Methods*; John Wiley: New York.
25. Shanks, D. (1955) Non-linear transformations of divergent and slowly convergent sequences. *Journal of Mathematical and Physical Sciences*, 34: 1.
26. Pedroso, R.I. and Domoto, G.A. (1973) Inward spherical solidification—solution by the method of strained coordinates. *International Journal of Heat and Mass Transfer*, 16 (5): 1037–1043.